Published in final edited form as:
J Neural Eng. 2011 August ; 8(4): 046001. doi:10.1088/1741-2560/8/4/046001.

High frequency stimulation abolishes thalamic network oscillations: an electrophysiological and computational analysis

Kendall H. Lee, M.D., Ph.D.[1], **Frederick L. Hitti**[2], **Su-Youne Chang, Ph.D.**[1], **Dongchul C. Lee, Ph.D.**[3], **David W. Roberts, M.D.**[4], **Cameron C. McIntyre, Ph.D.**[3], and **J.C. Leiter, M.D.**[2]

[1]Department of Neurologic Surgery, Mayo Clinic, 200 First Street SW, Rochester, MN, 55902

[2]Department of Physiology Dartmouth Medical School, One Medical Center Drive, Lebanon, NH 03756

[3]Department of Biomedical Engineering, Cleveland Clinic Foundation, 9500 Euclid Avenue ND20, Cleveland, Ohio 44195

[4]Department of Neurosurgery, Dartmouth Medical School, One Medical Center Drive, Lebanon, NH 03756

Abstract

Deep Brain Stimulation (DBS) of thalamus has been demonstrated to be an effective for treatment of epilepsy. To investigate mechanism of action of thalamic DBS, we examined the effects of high frequency stimulation (HFS) on spindle oscillations in thalamic brain slices from ferrets. We recorded intracellular and extracellular electrophysiological activity in the nucleus Reticularis thalami (nRt) and in thalamocortical relay (TC) neurons in the lateral geniculate nucleus, stimulated the slice using a concentric bipolar electrode, and recorded the level of glutamate within the slice. HFS (100 Hz) of TC neurons generated excitatory post-synaptic potentials (EPSPs), increased the number of action potentials in both TC and nRt neurons, reduced the input resistance, increased the extracellular glutamate concentration, and abolished spindle wave oscillations. High frequency stimulation of the nRt also suppressed spindle oscillations. In both locations, HFS was associated with significant and persistent elevation in extracellular glutamate levels and suppressed spindle oscillations for many seconds after the cessation of stimulation. We simulated HFS within a computational model of the thalamic network, and HFS also disrupted spindle wave activity, but the suppression of spindle activity was short-lived. Simulated HFS disrupted spindle activity for prolonged periods of time only after glutamate release and glutamate-mediated activation of a hyperpolarization-activated current (I_h) were incorporated into the model. Our results suggest that the mechanism of action of thalamic DBS as used in epilepsy may involve the prolonged release of glutamate, which in turn modulates specific ion channels such as I_h, decreases neuronal input resistance, and abolishes thalamic network oscillatory activity.

Keywords

high frequency stimulation (HFS); deep brain stimulation (DBS); spindle oscillations

Corresponding author: Kendall H. Lee, M.D., Ph.D., Department of Neurosurgery, Mayo Clinic, 200 First Street SW, Rochester, Minnesota 55905, Telephone: 507-284-2816; Fax: 507-284-5206, lee.kendall@mayo.edu.

Introduction

Though Deep Brain Stimulation (DBS) of thalamus has been demonstrated to be an effective for treatment of epilepsy (Fisher et al., 2010), the mechanism of action has been the subject of intense debate. It is now well known that certain subtype of epileptic seizures are associated with oscillatory phenomena in the thalamus. For example, absence seizure are associated with 3 Hz spike and wave oscillations in the EEG and are likely to represent a perverse form of thalamo-cortical activity that is related to the normal generation of spindle waves (McCormick and Contreras, 2001). Both spontaneous normal spindle and abnormal seizure-like activities are elicited by the harmonic balance between inhibitory action on glutamatergic thalamocortical relay (TC) neurons and excitatory action on GABAergic nucleus reticularis thalami neurons (nRt). As part of the normal formation of spindles, $GABA_A$ receptors on TC neurons are activated and generate inhibitory post-synaptic potentials (IPSPs) that last about 100 msec. When $GABA_A$ receptors are blocked with bicuculline, the duration of the IPSPs increases to about 300 msec due to activation of $GABA_B$ receptors (von Krosigk et al., 1993), and the oscillations slow to 3 Hz. Since the intrinsic harmonics of the TC cells (which oscillate preferentially at ~3 Hz) match that of the TC-nRt loop (which also oscillates preferentially at ~3 Hz), these 3 Hz bursts become very strong, and generate a massive synchronized discharge at about 3 Hz. In this manner, normal spindle waves *in vitro* can be 'perverted' into absence-seizure-like events even in an isolated brain slice. Surprisingly, these spontaneous normal spindle activity and abnormal absence-seizurelike activity can be obtained in ferret thalamic slices, even in a reduced brain preparation (von Krosigk et al., 1993). Thus, the ferret thalamic slice is an ideal model to test the functional role of DBS in modulating thalamic circuit dynamics (Lee and McCormick, 1996 and 1997; Lee et al., 2005a).

Using the ferret thalamic model, we have previously reported that high frequency stimulation (HFS) results in local glutamate release that could abolish spindle oscillations in TC neurons (Tawfik et al., 2010). However, the precise post-synaptic effect of the glutamate release on membrane potential, input impedance, ionic channels, and the neural network dynamics that disrupt oscillatory activity in the thalamus has not yet been explored. Here, to address these important issues, we investigated the extracellular and intracellular effects of HFS on both the activity of TC neurons and on GABAergic nRt neurons within an isolated brain slice preparation from the ferret thalamus. We assessed the HFS mediated changes in extracellular glutamate, intracellular input impedance changes, membrane potential changes, and modulation of an ionic conductance called hyperpolarization activated cation current (I_h) that is known to be modulated by glutamate (Nita et al., 2003; van Welie et al., 2004) and to play an integral role in abolishing thalamic spindle oscillation (Lee & McCormick, 1996; Destexhe & Sejnowski, 2003). Finally, we studied the effect of HFS within a computational model of thalamic neuronal circuits to explore the electrophysiological mechanism(s) whereby neurotransmitter release modulates I_h and abolishes synchronized oscillations. In both sets of studies, we tested the hypothesis that HFS results in release of glutamate, alter the electrophysiological behavior of TC and nRt neurons and thereby disrupt the oscillatory activity within the thalamic neural network.

Methods

Slice Preparation

Brain slices were prepared from 3–4 month old male or female ferrets (*Mustela putorious furo*; Marshall Farms; North Rose, New York). The animals were deeply anesthetized with sodium pentobarbital (30–40 mg/kg) and decapitated. The forebrain was rapidly removed, and the hemispheres were separated with a midline incision. Four hundred micron thick slices were cut in the sagittal plane using a vibratome (Ted Pella, Inc.). During preparation

of slices, the tissue was placed in a chilled (5° C) sucrose-substituted solutions, which NaCl in artificial cerebrospinal fluid (aCSF) was replaced with sucrose while maintaining an osmolarity of 307 mOsm to increase tissue viability (Aghajanian & Rasmussen, 1989). Slices were placed in an interface style recording chamber (Fine Sciences Tools, Foster City, CA) maintained at 34 ± 1° C and allowed at least two hours to recover. The bath was perfused with aCSF, which contained (in mM): NaCl, 126; KCl, 2.5; $MgSO_4$, 1.2; NaH_2PO_4, 1.25; $CaCl_2$, 2; $NaHCO_3$, 26; dextrose, 10 and was aerated with 95% O_2, 5% CO_2 at a final pH of 7.4. For the first 20 minutes of perfusion of the thalamic slices, the bathing medium contained an equal mixture of aCSF and the sucrose-substituted solution; subsequently, the perfusate was witched to aCSF alone. All chemicals were purchased from Sigma-Aldrich, Inc (St. Louis, MO).

Electrophysiology

Intracellular recording electrodes were pulled on a Sutter Instruments P-2000 laser micropipette puller from medium-walled glass (1B100F, World Precision Instruments, Sarasota, FL). Micro-pipettes were filled with 2 M K-acetate and had tip resistances of ~ 60–120 MegaΩ. Neurons within the slice were impaled, and activity was recorded in the bridge mode using an Axoclamp 2A amplifier (Axon Instruments), the data were filtered and analyzed using Axotape (Axon Instruments) on a PC style computer, and figures were drawn using CorelDRAW. The input resistance was measured by injecting hyperpolarizing current (100–300 ms, 0.1 – 0.6 nA, 1 Hz) into the neuron, and the amplifier bridge was balanced before each determination of input resistance. Only those neurons exhibiting a stable resting membrane potential less than or equal to −60 mV were included in the analysis. Electrical stimulation of the thalamus was achieved by placing a concentric bipolar stimulating electrode and delivering monophasic stimulation (100 μsec pulse width; 10–500 μA amplitude; 100 Hz frequency) using a Master 8 stimulator (A.M.P.I., Jerusalem, Israel).

Glutamate amperometry

An enzyme-based glutamate biosensor electrode (Pinnacle Technology, Inc., Lawrence, Kansas) was used to measure glutamate release (Hu et al., 1994; Tawfik et al., 2010), which had rapid response times (about 1 s) and high degree of sensitivity (less than 2 microM) and selectivity for L-glutamic acid (Hu et al., 1994). An interferent screening inner membrane coated the bare platinum-iridium electrode, and the enzyme layer was formed over the inner membrane by co-immobilizing glutamate oxidase and ascorbate oxidase with glutaraldehyde and bovine serum albumin. Glutamate biosensors were tested in 0.1 mol/L phosphate-buffered saline (PBS) (pH = 7.4) for a minimum glutamate sensitivity of 300 pA/μM and for insensitivity to ascorbate (response to 250 μM ascorbate less than 0.5 nA). Sensors that did not meet these criteria were rejected. The electrode was modified by the company to make the sensitive surface at the tip of the electrode flat (rather than cylindrical) with sensing region of approximately 350 μm and appropriate for brain slice work. The presence of glutamate changes the oxidation current at the tip of the electrode, and this change in current was recorded with a multi-channel potentiostat (Model 3104, Pinnacle Technology, Inc., Wyckoff, NJ) and displayed and analyzed using Pinnacle Acquisition Laboratory software (Pinnacle Technology, Inc.). These enzyme-based electrodes have response times of about 1 sec and high degree of sensitivity and selectivity for glutamate (Hu et al., 1994). Once the glutamate biosensor was in position, a fixed potential of +0.6 V was applied between the working and the integrated Ag/AgCl reference electrode. After the oxidation current reached relatively steady-state baseline levels, electrical stimulations were performed allowing on-line current monitoring during each stimulation period. Changes in oxidation current elicited by stimulations had a relatively slow time course and was low-pass filtered at 1 Hz. Pre-stimulation baseline to peak change in oxidation current was determined for every stimulation. Oxidation currents were converted to glutamate concentrations with a post-

experiment calibration performed with step-wise increases of known glutamate (Sigma-Aldrich, St. Louis, MO) concentration in a stirred beaker.

Data analysis

Mean values are given ± the standard error of the mean (SEM). Comparisons between treatment conditions were made using paired or unpaired t-tests as appropriate. A P-value ≤ 0.05 was set as the level of statistical significance.

Computer model

To asses the ionic mechanisms associated with HFS, we adapted a network model that was originally designed to accurately reproduce spindle oscillations observed in ferret thalamic slices (Destexhe et al., 1996). The model incorporates the interaction between TC and nRt neurons that results in spindle activity (Figure 7A) and was further developed in the NEURON simulation environment (Hines & Carnevale, 1997). Model oscillations were generated by the reciprocal connectivity and bursting properties of the TC and nRt cells. The network model used in this study consisted of four single compartment neurons with Hodgkin-Huxley type membrane dynamics (2 TC and 2 nRt neurons). The neuron models were interconnected with synaptic currents based on kinetic models of AMPA, $GABA_A$, and $GABA_B$ receptors, all of which are fully described in previous studies (Destexhe et al., 1994; Destexhe et al., 1996). In addition, to the traditional sodium and potassium channels responsible for action potential generation, the TC and nRt cells also contained low threshold calcium currents (T-type) and the TC cell incorporated a hyperpolarization activated cation current (I_h), which plays a key role in the waxing and waning pattern of spindle activity.

Modifications to the Computer Model

To simulate the direct effects of the electric field applied to the thalamic slice, intracellular suprathreshold current pulses were delivered to TC cell (100 μs pulses delivered at 100 Hz; Figure 7A). To simulate the indirect effects of extracellular stimulation, stimulation-induced release of exogenous glutamate was applied to the stimulated TC cell. Each stimulus pulse activated glutamate release in the model, which subsequently activated AMPA receptors in the postsynaptic TC cell. The diffusion and clearance kinetics of the stimulation-induced extracellular glutamate was modeled by:

$$\frac{dGlu_e}{dt} = Glu_e + \frac{(Glu_\infty - Glu_e)}{\tau_{Glu}},$$

where Glu_e is the extracellular glutamate concentration, Glu_∞ is the steady-state extracellular glutamate concentration, and τ_{Glu} is the time constant (1500 ms) of decay of the extracellular glutamate concentration. The parameters of this equation were fit to match the time course of the extracellular glutamate effects in our experimental results before, during, and after HFS (Figure 7C).

The I_h channel was represented with activation dynamics using a kinetic model for a calcium-induced shift in the activation voltage (Hagiwara & Irisawa, 1989; McCormick & Pape, 1990; Destexhe *et al*., 1993). The original I_h kinetic model had three different states ($C \Leftrightarrow O_1 \Leftrightarrow O_2$; C: closed, O_1: open and O_2: open with binding Ca) (Destexhe et al., 1993; Destexhe et al., 1996). Recent experimental data indicate that glutamate may also modulate I_h activation (Nita *et al*., 2003; Frere & Luthi, 2004; van Welie *et al*., 2004). Therefore, we incorporated glutamate-dependent activation of I_h in our model by increasing probability of

opening (O_2) directly from the C state ($C \Leftrightarrow O_1 \Leftrightarrow O_2 \Leftrightarrow C$) as a function of the extracellular glutamate concentration.

$$C \overset{\alpha,\beta}{\longleftrightarrow} O_2$$
$$\alpha = 1.5 \cdot 10^{-3} \cdot \frac{Glu_e}{Glu_\infty},\ \beta = 10^{-8},$$

where α and β are the forward and inverse rates between the C and O_2 states. In addition to incorporating glutamate modulation of I_h, minor modifications were made to the original Destexhe et al. (1996) model, to better match our model firing properties to our experimentally recorded spindle oscillations (Figure 7C). Changes to the TC cells included reducing the specific membrane capacitance to 0.9 μF/cm^2, increasing the maximum conductance of the fast Na channel to 0.16 S/cm^2, decreasing the Ca^{2+} diffusion rate to 3.5 ms, and shifting the voltage dependence of the Na, K, Ca_T currents by 10, 10, and −3 mV, respectively. The I_h channel had an adjusted equilibrium potential (−38 mV), reduced maximum conductance 8.12E-6 S/cm^2 in TC cell 1 and 9.57E-6 S/cm^2 in TC cell 2, and an adjusted unitless scaling factor for the rate constant from O_2 to O_1 (0.008) and power for computing for rate constant from O_1 to O_2 (1.5). These changes were not based on voltage-clamp studies of these cells, but were empirically guided by the improved fit of the model results to our experimental measurements.

Results

Spontaneous Spindle wave generation in relay and nRt neurons

Extracellular recordings were obtained from the lateral geniculate nucleus (LGN) while simultaneously recording intracellularly from glutamatergic TC neurons in the LGN (Figure 1A; n = 6 cells) or GABAergic nRt neurons in the perigeniculate nucleus (PGN) (Figure 1B; n = 5 cells). All the slices (n= 11) used demonstrated spontaneous spindle waves as previously reported (Von Krosigk et al., 1993). In the TC neuron, IPSPs were seen at 7–14 Hz, and in some cases the IPSPs were followed by rebound membrane depolarization, which presumably resulted from low threshold Ca^{2+} spikes (Bal et al., 1995a; Bal et al., 1995b). A burst of action potentials often followed the rebound depolarization. In the GABAergic nRt neurons, EPSPs were seen at 7–14 Hz and were associated with bursts of action potentials.

Extracellular recording during HFS

The effect of HFS on the spontaneous generation of spindle waves was studied by recording extracellular activity within the thalamic slice. Stimulation (duration ~4 sec, frequency 100 Hz, intensity 300 μA, pulse width 100 μsec) in the A1 lamina of the LGN while recording in the nRt ~600 μm anterior to the stimulating electrode abolished spindle wave activity for ~23 sec average (Figure 2A; n = 5 slices). Spontaneous spindle waves returned following this temporary cessation of activity. Stimulation of the LGN with the same parameters resulted in a ~28 sec average cessation of spindle wave activity recorded in the A1 lamina of the LGN ~100 μm from the stimulating electrode (Figure 2B; n = 5 slices). Similar effects were seen when the stimulating electrode was placed in the PGN. Stimulation of the nRt neurons in the PGN using the parameters listed above stopped spindling activity recorded extracellularly ~100 μm from the stimulating electrode in the PGN for an average of ~20 sec (Figure 2C; n = 5 slices). Stimulation of the nRt neurons in the PGN also stopped spindle wave activity for 29.2 ± 1.8 sec in the A1 lamina of the LGN ~600 μm posterior to the stimulating electrode (Figure 2D; n = 5 slices). Stimulation in the LGN or PGN was equally effective at disrupting spindle activity.

Intracellular effects of HFS on nRt neurons

The effects of HFS on individual GABAergic nRt neurons were also tested by recording intracellular activity. Stimulation (duration ~3 sec, frequency 100 Hz, intensity 300 μA, pulse width 100 μsec) was given in the A1 lamina of the LGN. The intracellular activity of individual nRt neurons, which all exhibited a stable resting membrane potential (V_m) of less than −60 mV (average V_m= −67.4 ± 2.0), was recorded ~600 μm anterior to the stimulating electrode. The GABAergic nRt neurons exhibited EPSPs at a frequency of 7–10 Hz (Figure 3a; n = 7 cells), which was the same frequency as the spontaneously occurring spindle waves (Von Krosigk *et al*., 1993; Bal *et al*., 1995a; Bal *et al*., 1995b; Steriade & Amzica, 1998). These EPSPs resulted in the firing of a burst of action potentials (Figure 3e; n = 7 cells). During the stimulation period, the neuron was significantly depolarized by ~12.0 ± 0.7 mV (Figure 3b and f; n = 7 cells; $P < 0.001$). Stimulation artifacts were also recorded in the intracellular trace during the stimulation period. When these artifacts were manually removed, the presence of tonic action potential firing due to the stimulation induced depolarization was detected (Figure 3f; n = 7 cells). Action potentials ceased in the nRt neurons before the termination of HFS. Moreover, stimulation temporarily abolished spindle wave activity in the GABAergic nRt neuron. After stimulation, the neurons returned to a resting V_m of −67.8 ± 1.8 mV, which was not significantly different from pre-stimulation values and did not exhibit a barrage of EPSPs characteristic of spindle wave generation for many seconds (Figure 3c; n = 7 cells). Spindle wave activity did not return for ~25 sec during which the neuron remained at resting membrane potential (Figure 3c; n = 7 cells). The post-stimulation spindle wave activity, once it was fully re-established, was indistinguishable from the spindle activity recorded before HFS was provided (Figure 3d).

Input resistance decreases during HFS in TC and nRt neurons

The effect of HFS on apparent input resistance was tested in both the glutamatergic TC neurons and GABAergic nRt neurons. The response of one TC neuron to the hyperpolarizing pulses used to measure input resistance is shown in Figure 4. In these neurons, the 0.6 nA square-wave current pulse hyperpolarized the membrane potential (Figure 4A). There was depolarizing sag, presumably due to I_h, and a rebound burst of action potentials occurred, probably due to activation of the low threshold calcium current (I_T) after the hyperpolarizing current was turned off (Figure 4F). HFS (duration ~2 sec, frequency 100 Hz, intensity 300 μA, pulse width 100 μsec) was delivered to the A1 lamina ~600 μm posterior to the intracellular recording electrode. During HFS, the hyperpolarizing current pulse resulted in less membrane hyperpolarization compared to before HFS was delivered (Figure 4B). Manual removal of the stimulation artifacts (Figure 4G) revealed that the depolarizing sag current and rebound bursting of action potentials were absent during the stimulation period. Additionally, a 5 mV sustained membrane depolarization and single action potential was recorded during HFS (Figure 4G). Immediately after HFS, the hyperpolarizing current pulse resulted in less membrane hyperpolarization compared to before HFS was delivered (Figure 4C), but the input resistance returned to the initial values ~6 sec after HFS stopped (Figure 4D). An overlay of the membrane responses to the hyperpolarizing current pulses before and immediately after HFS revealed a decrease in hyperpolarization in response to the current pulses (Figure 4E). In the TC neurons, the mean input resistance before HFS was 53.5 ± 3.7 MΩ, and the input resistance decreased significantly to 26.1 ± 2.6 MΩ during HFS (Figure 4H, n = 10 cells; $P < 0.001$).

We used a similar protocol to measure input resistance in the nRt neurons. Before HFS, hyperpolarizing current pulses (100–300 ms, 0.3 nA, 1 Hz) resulted in the membrane hyperpolarization of the nRt neuron (Figure 5A). During HFS, the current pulses resulted in less membrane hyperpolarization. With the stimulation artifacts manually removed from the intracellular recording, this decrease in hyperpolarization was readily apparent (Figure 5B).

Immediately following HFS, the hyperpolarizing current pulse also caused less membrane hyperpolarization compared to before HFS was delivered (Figure 5C), but the input resistance returned to its initial value within ~4 sec after HFS was stopped (Figure 5D). An overlay of the membrane responses to the hyperpolarizing current pulses, given before and immediately after HFS, displayed a decrease in the voltage drops due to HFS (Figure 5E). The mean input resistance in nRt neurons before HFS was 87.9 ± 14.8 MΩ, and the input resistance fell significantly during HFS to 61.3 ± 15.4 MΩ (Figure 5F; n = 5 cells; $P < 0.001$). Thus, input resistance was significantly higher in nRt cells compared to TC cells during either resting or stimulated conditions ($P < 0.007$), but HFS caused a similar significant drop in the input resistance in both cell types ($P < 0.001$).

Amperometry/glutamate electrode

The release of glutamate in response to HFS was measured directly with a glutamate specific biosensor. Release of glutamate was recorded as an increase in oxidation current as measured by the biosensor. HFS applied to the A1 lamina of the LGN (duration 5 or 10 sec, frequency 100 Hz, intensity 300 μA, pulse width 100 μsec) was followed by an increase in oxidation current in both the LGN and the PGN when the recording electrodes were placed ~100 μ m and ~600 μ m anterior to the stimulating electrode respectively (Figure 6A; n = 3 slices). The elevation of extracellular glutamate lasted on average 69.0 ± 3.3 sec after 5 sec of HFS. The duration of elevation of the extracellular glutamate concentration exceeded the duration of stimulation in all cases. The peak value of glutamate occurred on average 12.9 ± 1.8 sec after the onset of stimulation for stimulation durations of 5 sec, which was also after electrical stimulation had ceased. To test the area over which HFS induced glutamate release, the PGN recording electrode was moved ~500 μ m dorsally, and no change in oxidation current was recorded in response to HFS (Figure 6B, n = 3 slices). The measured increase in oxidation current is directly related to the amount of glutamate released, and the increase in oxidation current measured relative to the baseline unstimulated value in the LGN and PGN following HFS was equal to an increase of the glutamate concentration of 43 ± 7 μM (range 15–75 μM).

Computer model

The interaction between these intrinsic ionic currents in TC and nRt neurons and the network synaptic dynamics among neurons generated sustained spindle oscillations (Fig. 7B). The model network spindle oscillations closely match a wide range of experimental observations such as ~5 Hz bursting with 2–3 s period of spindle oscillation separated by 5~8 s (Destexhe *et al*., 1993; Destexhe & Sejnowski, 2003). Our implementation of this computational model of the TC-nRt network accurately reproduced the spindle oscillations that we observed experimentally in our preparation (Figure. 7B). Each spindle in the model was initiated by a hyperpolarizing current injection into TC cell 1. This hyperpolarizing current mimicked the inhibitory stimulation generated within the nRT that normally serves as the pacemaker for spindle activity (Steriade *et al*., 1985). Within each spindle, the two TC cells exhibited alternating bursting while both nRt neurons fired bursts on each spindle cycle. The time course of the transmembrane potentials, spikes per burst, burst frequency within spindles, spindle duration, and spindle frequency all closely matched our experimental recordings.

We assessed the capacity of the model, as originally described (Destexhe et al., 1996), to mimic the experimentally observed the effects of HFS on spindle activity. During and after HFS in the *in vitro* thalamic slice, spindle oscillations ceased, neuronal input impedance (R_{in}) decreased, and extracellular glutamate increased. When HFS was applied to the network model for 4 seconds, spindle oscillations were disrupted for the duration of the stimulation, but the model was unable to reproduce the decrease in R_{in} or the long duration

of spindle quiescence (~20–30 sec) that persisted even after HFS was terminated *in vitro* (contrast the *in vitro* data shown in Figure 2 with the simulated effect of HFS in Figure 7C). Thus, the originally described model could not replicate all of the experimentally observed features of HFS in the thalamic slice preparation.

In recent studies, modulation of I_h by glutamate has been described (Nita et al., 2003; van Welie et al., 2004), and I_h is known to play an integral role in the thalamic spindle oscillation (Destexhe & Sejnowski, 2003). Therefore, we incorporated glutamate-dependent activation of I_h in the TC cells, and reexamined the effect of HFS on spindle oscillations within the model. Once glutamate-dependent modulation of I_h was added to the model, simulated HFS to TC cell 1 stopped the spindle oscillation for ~20 s after termination of HFS (Figure 7C), and the R_{in} during HFS was decreased to almost half of the steady-state (or inter-spindle state) value; results that are similar to our actual experimental findings. However, the model did not reproduce the experimentally recorded decreased R_{in} during the post-stimulation phase of quiescence before the spindle oscillations resumed.

Our *in vitro* experiments also showed that HFS applied to the nRt stopped spindle oscillations and increased the extracellular glutamate concentration within the thalamus. HFS of the nRt in our model, ignoring glutamate modulation of I_h in the TC cells, was unable to generate the period of spindle quiescence that followed HFS of nRt neurons in the slice preparation. However, spindle oscillations could be stopped in our model when simulated glutamate release and subsequent I_h modulation was applied to a TC cell in combination with the HFS of a nRt neuron. The duration of the spindle quiescence in the model closely matched our experimental recordings (data not shown).

Discussion

Although it has been previously demonstrated that HFS results in release of local glutamate release and suppression of spindle oscillations in the thalamic slice (Tawfik et al., 2010), the precise post-synaptic effect of the glutamate release on membrane potential, input resistance, ionic conductance such as I_h, and the neural network dynamics that disrupt oscillatory activity such as seizures and spindle waves in the thalamus is unknown. The novel findings of current study are as follows: 1. HFS to either thalamocortical relay or nRT neurons disrupted spindle wave activity indicating modulation of any node in the neural network responsible for network oscillatory activity has the potential to affect the whole network. 2. HFS results in depolarization of membrane potential, significant decreases in apparent input resistance, and abolished spindle wave generation in both nRT and TC neurons. The suppression of oscillatory neuronal activity lasted much longer than the duration of HFS. 3. Glutamate was released during and after HFS in both LGN and PGN. 4. The introduction of HFS into an established computational model of spindle wave activity suppressed spindle wave activity, but the suppression lasted only as long as the HFS. Prolonged suppression of spindle activity, which replicated our experimental observations, was achieved within our modified model only after HFS-induced glutamate release and glutamate modulation of I_h were incorporated into the model. Thus, glutamate release elicited by HFS appears to affect thalamic oscillatory activity by modulation of I_h, which lasts much longer than the duration of HFS, and may mediate the suppression of pathological oscillatory activity within the thalamus.

High frequency stimulation disrupts spindle wave generation

The circuit that generates spindle waves, 1–3 second epochs of synchronized 7–14 Hz oscillations, depends on the generation of a burst of action potentials in GABAergic nRt neurons, which causes IPSPs in TC neurons and hyperpolarizes the membrane potential by 2–10 mV (Von Krosigk *et al*., 1993; Bal *et al*., 1995a; Bal *et al*., 1995b; Steriade & Amzica,

1998). A subset of the glutamatergic TC neurons generate rebound low threshold Ca^{2+} spikes following the membrane hyperpolarization associated with the IPSPs, and a burst of action potentials is generated that returns to the nRt neurons as a barrage of EPSPs. This barrage of EPSPs activates a low threshold Ca^{2+} spike in the nRt neurons and initiates the next cycle of the spindle wave.

High frequency stimulation in the region of the nRT cells or TC cells *in vitro* initially elicits EPSPs and a series of action potentials (Figure 3) (Anderson *et al*., 2004; Lee *et al*., 2005a). The action potentials are followed by a period of depolarization block, and as a consequence, the elicited action potentials cease before HFS is terminated. In addition, HFS has a net depolarizing effect in both the nRt and TC cells (see Figure 3 and Anderson et al., 2004; Lee et al., 2005a). Spindle activity was suppressed by HFS and the cessation of spindle activity persisted after HFS had stopped. Thus, HFS seemed to cause initial excitation, but subsequent inhibition of neuronal activity within the slice. The depolarization of TC neurons occurring shortly after HFS begins probably abolishes spindle wave oscillations by inhibiting the rebound responses that are required to drive nRt neurons to discharge in synchrony. However, after cessation of HFS, the membrane potential slowly returned to lower levels, but spindle activity did not immediately resume. The I_h current is activated relatively slowly during periods of depolarization, presumably as a result of accumulation of intracellular Ca^{2+} during the period of depolarization. Augmented activity of I_h depolarizes the membrane potential and prevents deinactivation of the low threshold calcium current, and spindle activity is suppressed (Lee and McCormick, 1996; Destexhe *et al*., 1993). As calcium is removed or sequestered from the intracellular space, I_h activity is diminished, and spindle activity resumes. In the ferret slice preparation, spontaneous spindle waves occur with inter-spindle intervals of 7–25 sec, and there is a refractory period after each burst of spindles during which electrical stimulation fails to elicit a new sequence of spindle waves. The refractory period ranges from 7–14 sec (Kim et al., 1995). A similar period of refractoriness is likely to follow HFS and probably reflects the augmented activity of I_h immediately after HFS.

However, spindle activity did not resume until 20–30 seconds after HFS stopped, and this exceeds the expected refractory period. Therefore, some additional factor must account for the later stages of the quiescent period following HFS. It seems likely that this long duration process is associated with enhanced channel activity since the input resistance was reduced during the prolonged suppression of spindle activity that followed HFS. We studied glutamate release within the ferret thalamic slice using an enzyme-linked biosensor in which glutamate oxidase within the electrode catalyzed the oxidation of glutamate and released hydrogen peroxide, which was detected by a platinum/iridium electrode. Regardless of the site of stimulation within the slice, PGN or LGN, HFS elicited significant glutamate release, and the concentration of glutamate remained elevated for more than 60 seconds. The peak increase in glutamate was ~40 μM above the baseline control value. This concentration is well within the estimates of extrasynaptic glutamate concentrations in other systems (Dzubay & Jahr, 1999). Thus, the additional factor responsible for suppression of spindle activity is probably the elevated concentration of extracellular glutamate elicited by HFS.

The extracellular glutamate concentration depends on the rate at which glutamate is released and the rate at which it is taken up. The glutamate in our experiment may have originated from three sources within the slice. First, axons of corticothalamic projections remain in the slice and these projections are primarily glutamatergic (Deschênes & Hu, 1990). Second, the TC neurons themselves are glutamatergic. Third, astrocytes may release glutamate (Araque et al., 2000; Haydon, 2001). During the initial period of HFS, action potentials were elicited, and these may have stimulated glutamate release from TC cells, but it seems unlikely that glutamate was released from the TC cells during the period of depolarization block and

subsequent electrophysiological quiescence. Axons may be stimulated at high rates for prolonged periods of time (Ranck, 1975; McIntyre *et al*., 2004a), but here as well, it seems unlikely that synaptic release of glutamate persisted in axons once the HFS ceased. Astrocytic release of glutamate depends on oscillations of intracellular Ca^{2+} that are generated with slower time constants than neural events (Innocenti et al., 2000; Araque et al., 2001), and the release of glutamate from astrocytes may have persisted after HFS ceased. In our published studies (Tawfik et al., 2010), we found that glutamate release elicited by HFS was not inhibited by TTX (the source is, therefore, non-neuronal at least in part), and direct electrical stimulation of astrocytes in culture leads to calcium waves and glutamate release that can be inhibited by treatment with the calcium chelator, BAPTA (Lee et al., 2005b; Tawfik et al., 2010). Thus astrocytes may be an important source of glutamate during and after HFS, and therefore, an important therapeutic target for HFS. Finally, the level of glutamate will also depend on the rate of clearance of glutamate. The rate of glutamate clearance depends mainly on the activity of two excitatory amino acid transporters (EAAT1 and EAAT2 in humans), which are expressed predominantly in astrocytes. Depolarizing astrocytes slows glutamate uptake (Hansson et al., 2000), and astrocytes may be depolarized by direct effects of HFS or indirectly by an increase in extracellular potassium associated with the neuronal activity elicited by HFS.

Ionic Mechanisms Underlying Abolition of Thalamic Oscillations by HFS

Glutamate release elicited by HFS has the appropriate temporal profile to explain the relatively long lasting suppression of spindles in the slice. Thus, it is our hypothesis that the HFS mediated elevation of extracellular glutamate activates the post-synaptic glutamate ionotropic and metabotropic receptors in TC neurons and results in glutamate modulation of I_h. The modulation of I_h leads to membrane depolarization, preventing deinactivation of low threshold calcium currents and prevents the reciprocal cycles of excitation and inhibition between TC and nRt neurons that generate spindle waves. In addition, the activation of glutamate receptors and I_h may be responsible for the reduction in input resistance that we measured in the post-HFS interval before spindle activity resumed. However, important methodological differences between the HFS of the thalamic slices as used in the current study to DBS as used clinically in humans *in vivo* must be recognized. For example, we used concentric bipolar electrodes as apposed to the in-line type of electrodes used in humans, monophasic stimulation as apposed to biphasic stimulation, and constant current stimulation rather than constant voltage stimulation. Importantly, we have recently reported that monophasic electrical stimulation-induced glutamate release that was linearly dependent on stimulation frequency, intensity and pulse width in the anesthetized rat thalamus (Agnesi et al., 2010). Glutamate release was less pronounced with voltage-controlled stimulation and the efficacy of monophasic voltage-controlled stimulation, in terms of evoking glutamate release in the thalamus, was substantially higher when compared with biphasic (charge balanced) current-controlled stimulation (Agnesi et al., 2010). However, it remains to be determined whether similar glutamate release occurs with human DBS electrodes with charge balanced stimulation.

Computer model

To test our mechanistic hypothesis, we implemented an established computational model of spindle activity (Destexhe et al., 1996) and assessed the effects of HFS within this model. The original computer model was not able to replicate three key features of our experimental results: the extracellular glutamate concentration did not change in the model; the suppression of spindle activity within the model was short-lived compared to our experimental findings; and there was no reduction in R_{in} during the inter-spindle interval after HFS. The failure of the original model to replicate our experimental findings implies that some synaptic and/or ionic mechanisms associated with channel opening in the inter-

spindle interval were missing from the model. Therefore, we added glutamate release and clearance, coupled to glutamate-dependent activation of I_h, as suggested by previous experimental recordings (van Welie et al., 2004). These additions to the model led to prolonged suppression of spindle activation and a reduction in R_{in} during HFS. The changes to the model did not, however, exactly replicate our input resistance measurements following HFS. The model R_{in} returned to baseline more quickly than in the actual experimental study. It may be that we underestimated the extent of activation of I_h in the inter-spindle period or, more likely, we did not include other effects of glutamate on ionotropic glutamate receptors in TC and nRt cells that would prolong the reduction of R_{in}.

Limitations of Computer model

The computer model used in this study has limitations that should be noted. First, it must be recognized that, although the use of an established computer model to study the effect of DBS on thalamic spindle oscillations is useful as demonstrated here, fitting the model (by adding a glutamatergic mechanism for the I_h) to the data and then using this modified model to explain the data represents only one of the possible mechanism of effect and does not prove the actual mechanism. Second, our kinetic model of the glutamate- I_h interaction is not a quantitative representation validated by experimental observation. The mechanism was simply a hypothetical kinetic model incorporating the potential interaction between glutamate and I_h channels during HFS on the TC-nRt network. Moreover, the rate constants of glutamate release and uptake were chosen to match the period of post-HFS quiescence rather than the actual glutamate concentrations we measured. The glutamate levels that we measured remained elevated beyond the period of spindle quiescence, although the glutamate levels were declining as spindle activity resumed. It may be that the effective glutamate concentration at the glutamate binding site on or near I_h was lower or decayed faster than the extracellular measurements at the electrode tip. Alternatively, if the receptor(s) responsible for the effect of glutamate inactivate or are desensitized then the extracellular concentration of glutamate will not accurately reflect the actual timing of the glutamate effect. None of these complexities was incorporated into the model.

Conclusion

High frequency stimulation may suppress spindle activity by multiple mechanisms that evolve through time during and after HFS. In the early stages of HFS, spindles are disrupted by excitation and subsequent depolarization of TC and nRt neurons. After HFS ceases, a refractory period exists that may depend on a rise in intracellular calcium within the TC or nRt neurons, but later a glutamate dependent activation of I_h may develop and suppress spindle activity beyond the refractory period. HFS at either the LGN or PGN abolished spindle waves at both locations. Thus, it is likely that HFS given to any location within the thalamic network will affect the entire network. Oscillatory behavior within a computational model of the thalamic neural network was also disrupted by simulated HFS with a temporal profile matching our experimental results, but only after we added glutamate release and glutamate-dependent activation of I_h. Thus, HFS stimulation disrupts the rhythmic activity of the thalamus by an initial excitatory mechanism, but subsequently inhibitory processes develop that may depend on neurotransmitter release elicited by HFS. Thus, HFS is neither primarily inhibitory nor excitatory, but rather disruptive of the network oscillations that generate pathological behaviors. Finally, we identified HFS-mediated neurotransmitter release may originate in part from astrocytes (Tawfik et al., 2010), and to some extent the increased extracellular glutamate originates from astrocytes, astrocytes represent an unappreciated target of HFS and may play an important role in the prolonged dynamic response to HFS.

Acknowledgments

This work was supported by NIH (K08 NS 52232 award to KHL) and Mayo Foundation (Research Early Career Development Award for Clinician Scientists award to KHL).

References

Aghajanian GK, Rasmussen K. Intracellular studies in the facial nucleus illustrating a simple new method for obtaining viable motoneurons in adult rat brain slices. Synapse. 1989; 3:331–338. [PubMed: 2740992]

Agnesi F, Blaha C, Lin J, Lee K. Local glutamate release in the rat ventral lateral thalamus evoked by high-frequency stimulation. J Neural Eng. 2010; 7(2):26009. [PubMed: 20332553]

Anderson T, Hu B, Pittman Q, Kiss ZHT. Mechanisms of deep brain stimulation: an intracellular study in rat thalamus. J Physiol. 2004; 559(1):301–313. [PubMed: 15218068]

Araque A, Carmingoto G, Haydon PG. Dynamic signaling between astrocytes and neurons. Ann Rev Physiol. 2001; 63:795–813. [PubMed: 11181976]

Araque A, Li N, Doyle RT, Haydon PG. SNARE protein-dependent glutamate release from astrocytes. J Neurosci. 2000; 20:666–673. [PubMed: 10632596]

Bal T, von Krosigk M, McCormick DA. Role of the ferret perigeniculate nucleus in the generation of synchronized oscillations in vitro. J Physiol (Lond). 1995a; 483:665–685. [PubMed: 7776250]

Bal T, Von Krosigk M, McCormick DA. Synaptic and membrane mechanisms underlying synchronized oscillations in the ferret lateral geniculate nucleus in vitro. J Physiol (Lond). 1995b; 483:641–663. [PubMed: 7776249]

Benazzouz A, Piallat B, Pollack P, Benabid AL. Responses of substantia nigra pars reticulata and globus pallidus complex to high frequency stimulation of the subthalamic nucleus in rats: electrophysiological data. Neurosci Lett. 1995; 189:77–80. [PubMed: 7609923]

Deschênes M, Hu B. Electrophysiology and pharmacology of cortocithalamic input in neurons of the lateral thalamic nuclei: an intracellular study in the cat. Eur J Neurosci. 1990; 2:140–152. [PubMed: 12106057]

Destexhe A, Bal T, McCormick DA, Sejnowski TJ. Ionic mechanisms underlying synchronized oscillations and propagating waves in a model of ferret thalamic slices. J Neurophysiol. 1996; 76:2049–2070. [PubMed: 8890314]

Destexhe A, Mainen ZF, Sejnowski TJ. An efficient method of computing synaptic conductances based on a kinetic model of receptor binding. Neural Comput. 1994; 6:10–14.

Destexhe A, McCormick DA, Sejnowski TJ. A model for 8–10 Hz spindling in interconnected thalamic relay and reticularis neurons. Biophys J. 1993; 65 2473-2377.

Destexhe A, Sejnowski TJ. Interactions between membrane conductances underlying thalamocortical slow-wave oscillations. Physiol Rev. 2003; 83:1401–1453. [PubMed: 14506309]

Dzubay JA, Jahr CE. The concentration of synaptically released glutamate outside of the climbing fiber-porkinje cell synaptic cleft. J Neurosci. 1999; 19:5265–5274. [PubMed: 10377338]

Fisher R, Salanova V, Witt T, Worth R, Henry T, Gross R, et al. Electrical stimulation of the anterior nucleus of thalamus for treatment of refractory epilepsy. Epilepsia. 2010

Frere SG, Luthi A. Pacemaker channels in mouse thalamocortical neurones are regulated by distinct pathways of cAMP synthesis. J Physiol (Lond). 2004; 554:111–125. [PubMed: 14678496]

Garcia L, Audin J, D'Alessandro G, Bioulac B, Hammond C. Dual effect of high-frequency stimulation on subthalamic neuron activity. J Neurosci. 2003; 23:8743–8751. [PubMed: 14507974]

Hagiwara N, Irisawa H. Modulation by intracellular Ca^{2+} of the hyperpolarization-activated inward current in rabbit single sino-atrial node cells. J Physiol (Lond). 1989; 409:121–141. [PubMed: 2479735]

Hansson E, Muyderman H, Leonova J, Allansson L, sinclair J, Blomstrand F, Thorlin T, Nilsson M, Rönnbäck L. Astroglia and glutamate in physiology and pathology: aspects on glutamate transport, glutamate-induced cell swelling and gap-junction communication. Neurochem Intl. 2000; 37:317–329.

Haydon PG. Glia: Listening and talking to the synapse. Nature Rev. 2001; 2:185–193.

Hines ML, Carnevale NT. The NEURON simulation environment. Neural Comp. 1997; 9:1179–1209.

Hu Y, Mitchell KM, et al. Direct measurement of glutamate release in the brain using a dual enzyme-based electrochemical sensor. Brain Res. 1994; 659(1–2):117–125. [PubMed: 7820652]

Innocenti B, Parpura V, Haydon PG. Imaging extracellular waves of glutamate during calcium signaling in cultured astrocytes. J Neurosci. 2000; 20:1800–1808. [PubMed: 10684881]

Kim U, Bal T, McCormick DA. Spindle waves are propagating synchronized oscillations in the ferret LGNd in vitro. J Neurophysiol. 1995; 74:1301–1323. [PubMed: 7500152]

Lee KH, McCormick DA. “Abolition of spindle oscillations by serotonin and norepinephrine in the ferret lateral geniculate and perigeniculate nuclei in vitro.”. Neuron. 1996; 17(2):309–321. [PubMed: 8780654]

Lee KH, Blaha CD, Harris B, Cooper S, Hitti FL, Leiter JC, Roberts DW, Kim U. Dopamine efflex in the rat striatum evoked by electrical stimulation of the subthalamic nucleus: potential mechanism of action in Parkinson's disease. Eur J Neurosci. 2006; 23:1005–1014. [PubMed: 16519665]

Lee KH, Chang S-Y, Roberts DW, Kim U. High frequency stimulation of subthalamic nucleus results in neurotransmitter release. J Neurosurg. 2004

Lee KH, Hitti F, Shalinsky MH, Kim U, Leiter JC, Roberts DW. Abolition of spindle oscillation and 3 Hz absence seizure-like activity in the thalamus by deep brain stimulation: potential mechanism of action. J Neurosurg. 2005a; 103:538–545. [PubMed: 16235687]

Lee, KH.; Hitti, FL.; Tawfik, VL.; Kristic, KJ.; Harris, BT.; Leiter, JC.; Roberts, DW. Abstract Viewer/Itinerary Planner. Washington, D.C: Society for Neuroscience; 2005b. High - frequency stimulation abolishes network oscillations by astrocytic glutamate release. Program No. 898.2. In

Lenz FA, Normand SL, Kwan HC, Andrews D, Rowland LH, Jones MW, Seike M, Lin YC, Tasker RR, Dostrovsky JO, et al. Statistical prediction of the optimal site for thalamotomy in parkinsonian tremor. Mov Disord. 1995; 10:318–328. [PubMed: 7651450]

Lozano AM, Dostrovsky JO, Chen RC, Ashby P. Deep brain stimulation for parkinson's disease: disrupting the disruption. Lancet Neurol. 2002; 1:225–231. [PubMed: 12849455]

Magarinos-Ascone C, Pazo JH, Macadar O, Buno W. High-frequency stimulation of the subthalamic nucleus silences subthalamic neurons: a possible cellular mechanism in Parkinson's disease. Neuroscience. 2002; 115:1109–1117. [PubMed: 12453483]

McCormick DA, Contreras D. On the cellular and network bases of epileptic seizures. Annu Rev Physiol. 2001; 63:815–846. [PubMed: 11181977]

McCormick DA, Pape H-C. Properties of a hyperpolarization-activated cation current and its role in rhythmic oscillation in thalamic relay neurones. J Physiol (Lond). 1990; 431:291–318. [PubMed: 1712843]

McIntyre CC, Mori S, Sherman DL, Thakor NV, Vitek JL. Electrical field and stimulating influence generated by deep brain stimulation of the subthalamic nucleus. Clin Neurophysiol. 2004a; 115:589–595. [PubMed: 15036055]

McIntyre CC, Savasta M, Kerkerian-Le Goff L, Vitek JL. Uncovering the mechanism(s) of action of deep brain stimulation: activation, inhibition, or both. Clin Neurophysiol. 2004b; 115:1239–1248. [PubMed: 15134690]

Meissner W, Harnack D, Reese RE, Paul G, Reum T, Ansorge M, Kusserow H, Winter C, Morgenstern R, Kupsch A. High-frequency stimulation of the subthalamic nucleus enhances striatal dopamine release and metabolism in rats. J Neurochem. 2003; 85:601–609. [PubMed: 12694386]

Nita DA, Steriade M, Amzica F. Hyperpolarization rectification in cat lateral geniculate neurons modulated by intact corticothalamic projections. J Physiol (Lond). 2003; 552:325–332. [PubMed: 12937283]

Ranck JB. Which elements are excited in electrical stimulation of mammalian central nervous system: a review. Brain Res. 1975; 98:417–440. [PubMed: 1102064]

Steriade M, Amzica F. Coalescence of sleep rhythms and their chronolgy in corticothalamic networks. Sleep Res Online. 1998; 1:1–10. [PubMed: 11382851]

Steriade M, Deschênes M, Domich L, Mulle C. Abolition of spindle oscillations in thalamic neurons disconnected from nucleus reticularis thalami. J Neurophys. 1985; 54:1473–1497.

Tawfik V, Chang S, Hitti FL, Roberts DW, Leiter JC, Jovanovic S, Lee KH. Deep brain stimulation results in local glutamate and adenosine release: investigation into the role of astrocytes. Neurosurgery. 2010; 67(2):367–375. [PubMed: 20644423]

van Welie I, van Hooft JA, Wadman WJ. Homeostatic scaling of neuronal excitability by synaptic modulation of somatic hyperpolarization-activated Ih channels. Proc Natl Acad Sci. 2004; 101:5123–5128. [PubMed: 15051886]

Von Krosigk M, Bal T, McCormick DA. Cellular mechanisms of a synchronized oscillation in the thalamus. Science. 1993; 261:361–364. [PubMed: 8392750]

Windels F, Bruet N, Poupard A, Feuerstein C, Bertrand A, Savasta M. Influence of the frequency parameter on extracellular glutamate and gamma-aminobutyric acid in substantia nigra and globus pallidus during electrical stimulation of subthalamic nucleus in rats. J Neurosci Res. 2003; 72:259–267. [PubMed: 12672001]

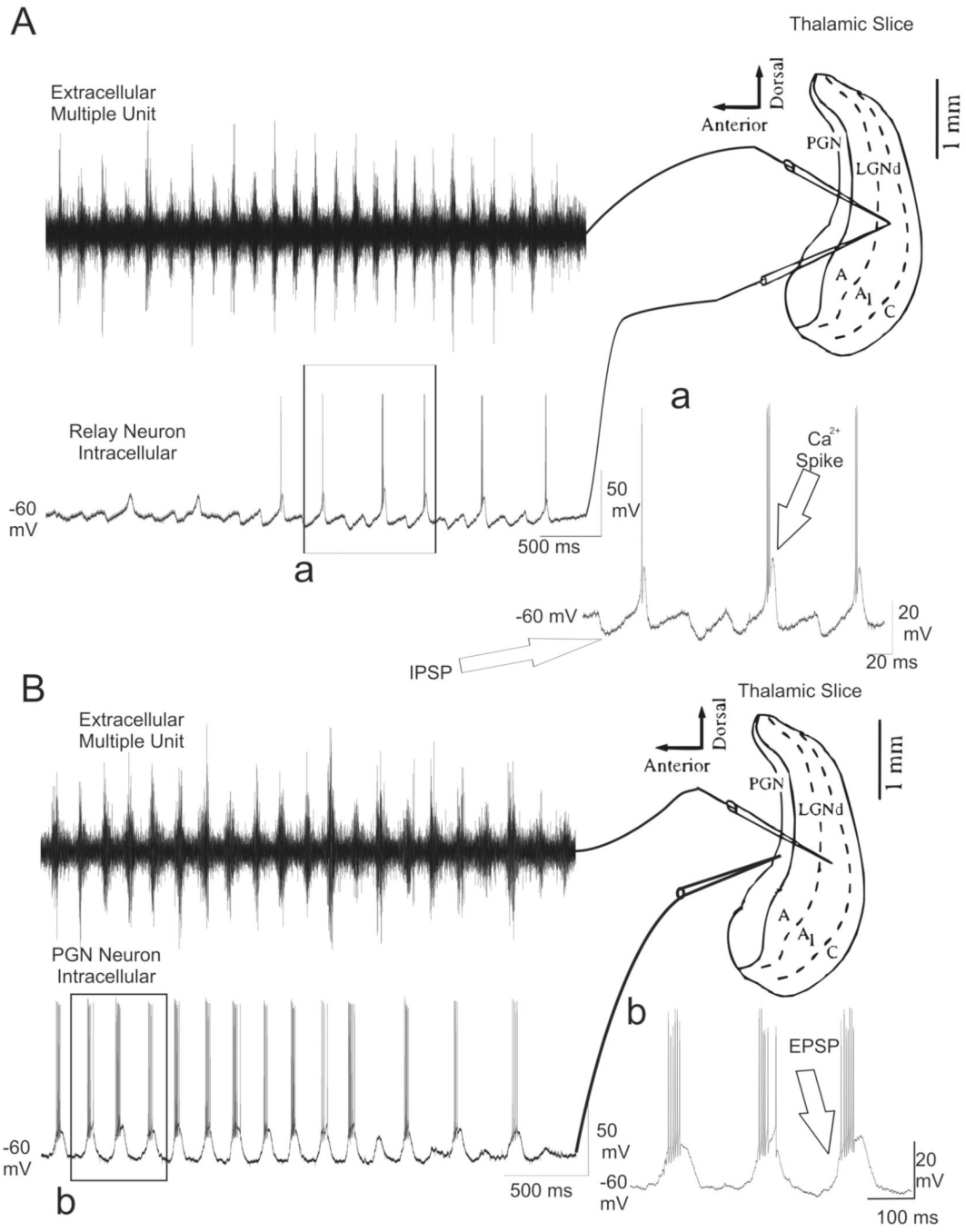

Fig. 1.

Simultaneous extracellular and intracellular recordings during spindle waves. (A) Spindle waves which were synchronized at 7–14 Hz oscillations were recorded extracellularly (left upper) and intracellularly (left down) in the A1 lamina of the ferret LGN (n= 6). In the thalamocortical relay (TC) neuron in the LGN, IPSP were seen at 7– 14 Hz, some of which resulted in rebound Ca^{2+} spikes and a burst of action potential (Aa). (B) Simultaneous extracellular recording (left upper) of the activity in A1 lamina while recording intracellularly (left down) from a GABAergic nRt neuron in the PGN (n= 5). EPSPs were seen at 7–14 Hz with resultant burst of action potentials (Bb).

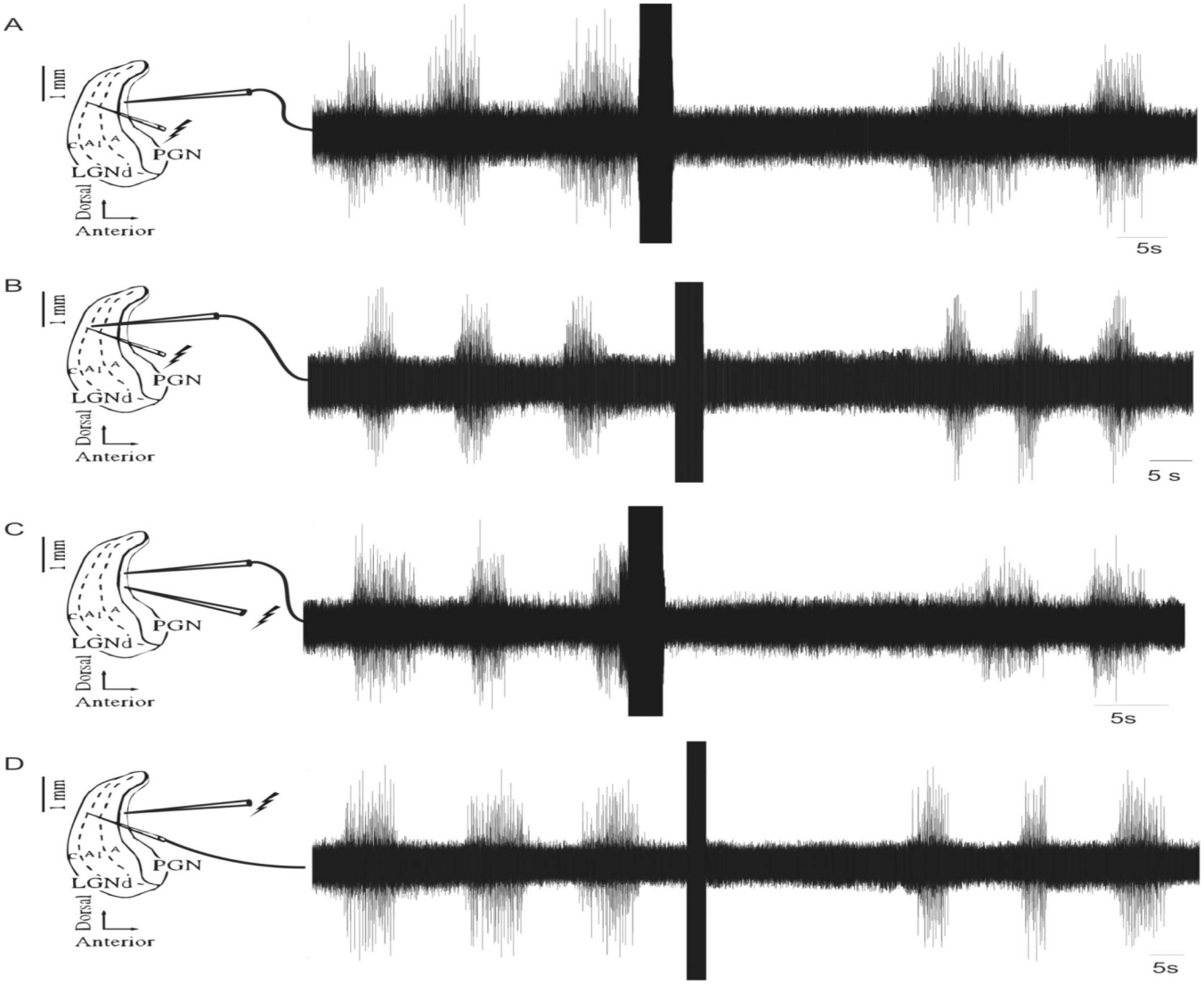

Fig. 2.

Extracellular recordings during HFS on thalamic slices exhibiting spontaneous spindle wave activity. (A) HFS (duration ~4 sec, frequency 100 Hz, intensity 300 μA, pulse width 100 μsec) applied to the A1 lamina of the LGN abolished spindle wave activity in the PGN for 22.6 ± 1.8 sec (n= 5 slices). (B) HFS with the aforementioned parameters resulted in a 26.6 ± 1.9 sec abolition of spindle wave activity recorded in ~100 μm from the stimulating electrode (n= 5 slices). (C) HFS of the PGN with the parameters listed above resulted in the cessation of spindling for 23.8 ± 2.4 sec as recorded ~100 μm from the stimulating electrode (n= 5 slices). (D) HFS in the PGN resulted in a ~27 sec long cessation of spindle wave activity ~600 μm posterior to the stimulating electrode (n= 5 slices).

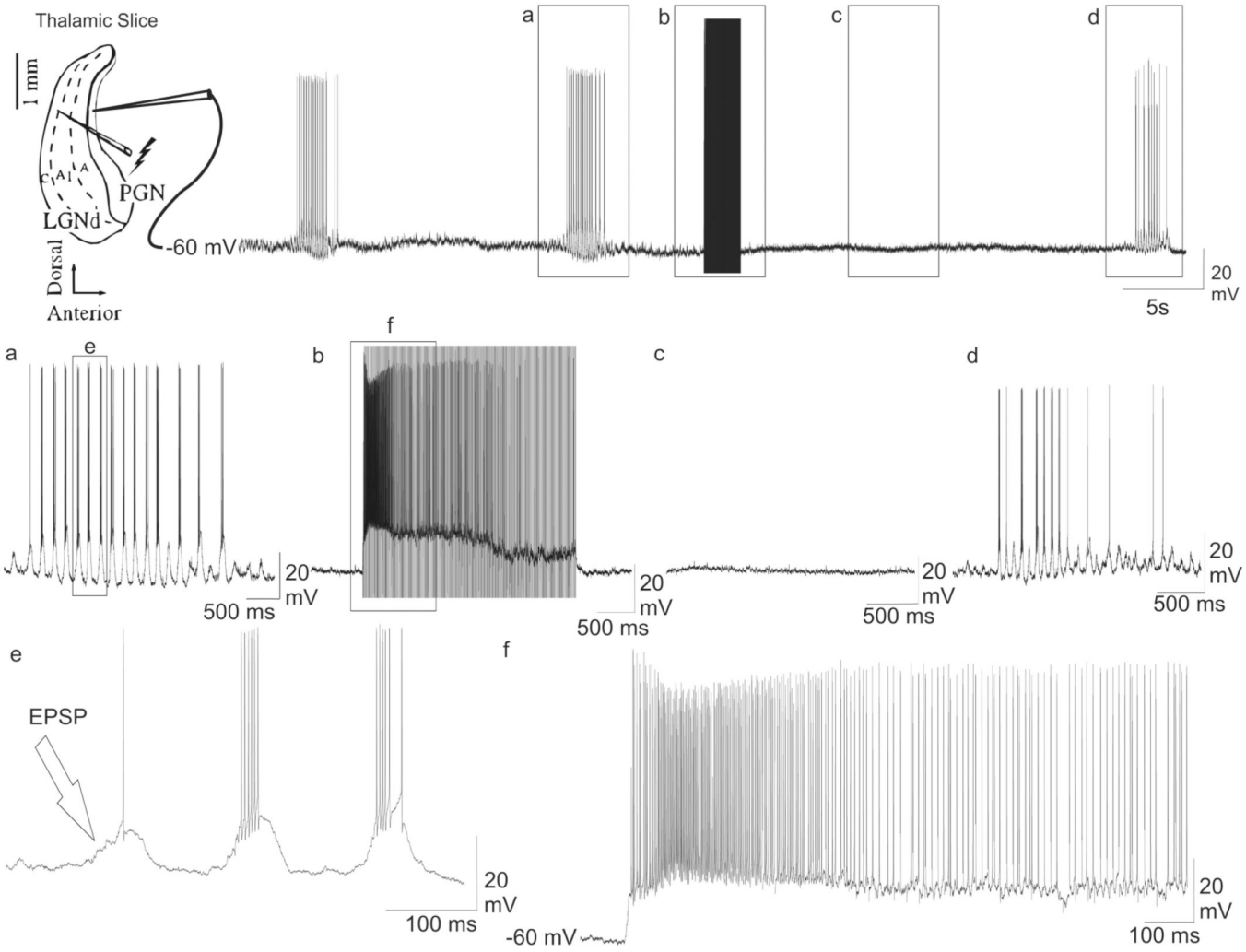

Fig. 3.

Intracellular recording from a nRt neuron in the PGN while the HFS was applied in the A1 lamina. Stimulation electrode was placed approximately 600 μm posterior to the recording electrode. The top trace presents the representative current clamp recording for the whole time period. (a) Magnification of a segment in the top trace showing a single spindle wave. (b) Enlargement of a segment of the top trace during HFS (duration ~3 sec, frequency 100 Hz, intensity 300 μA, pulse width 100 μsec). (c) Enlargement of a segment in the top trace showing absence of spindle wave following HFS. (d) Blow up of segment in the top trace showing the return of spontaneous spindle wave. (e) Enlargement of segment in a showing spontaneous EPSP's and burst of action potentials during a spindle wave. (f) Enlargement of segment in (b), with the stimulation artifacts manually removed, showing the effects of HFS during stimulation. HFS resulted in immediate membrane depolarization, action potential generation, and the abolition of spindle waves.

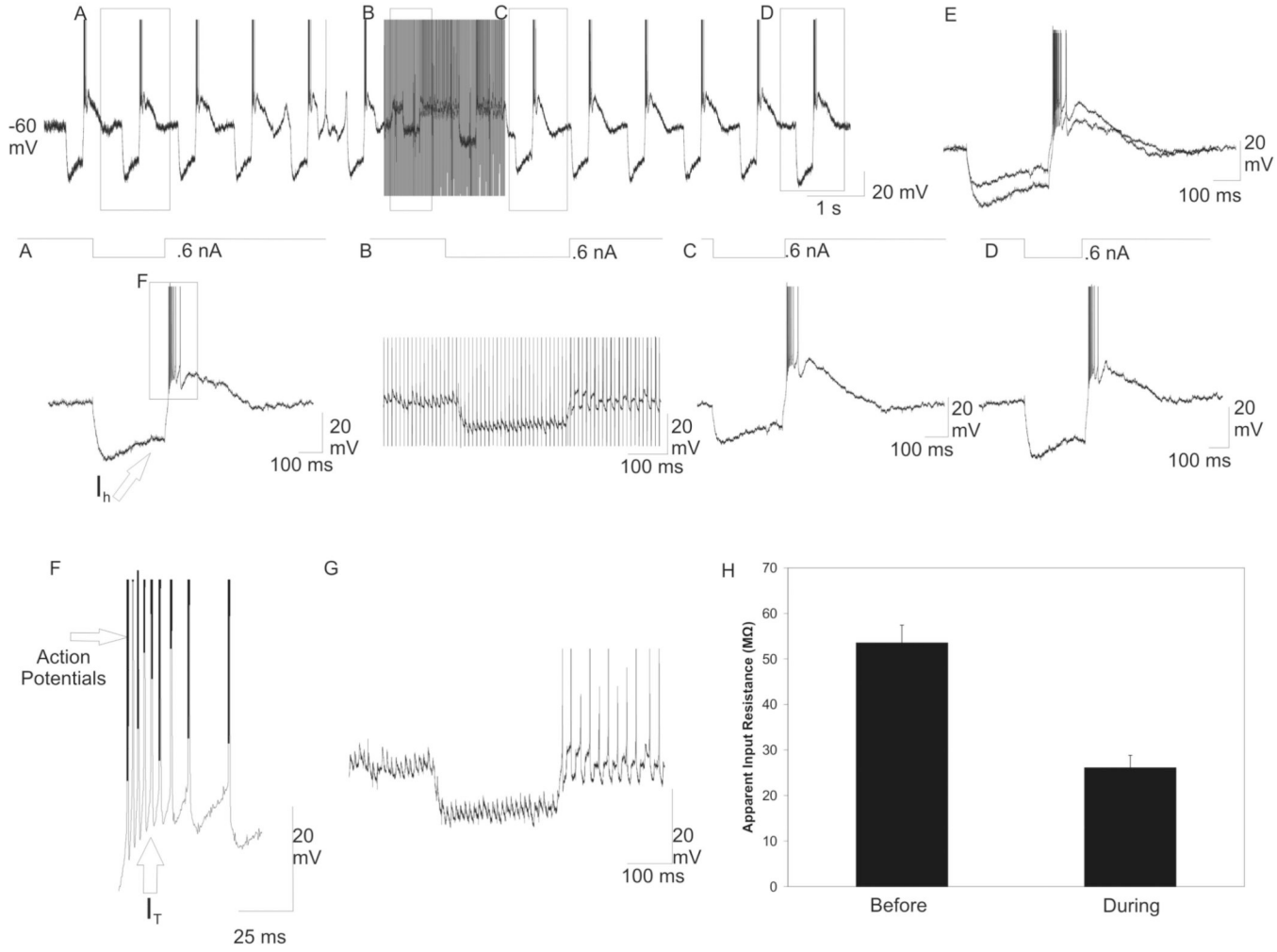

Fig. 4.

Decrease in the apparent input resistance with HFS in A1 lamina in a thalamocortical relay neuron in the A1 lamina. Intracellular recording from a TC neuron during HFS while hyperpolarizing square-wave current pulses (300 ms, 0.6 nA, 1 Hz) are delivered intracellularly to the recorded neuron. (A) Before HFS, the 0.6 nA hyperpolarizing current pulse resulted in membrane hyperpolarization, a depolarizing sag due to hyperpolarization activated cation current (I_h), and a rebound burst of action potentials due to presumed I_T activation upon turning off the current pulse. (B) Magnification of the labeled portion of the top trace. During HFS, there was 5 mV sustained membrane depolarization and single spike action potential generation. The hyperpolarizing current pulse resulted in significantly less membrane hyperpolarization compared to pre-HFS hyperpolarizing current pulse. There was also an absence of sag current and rebound bursting. (C) Enlargement of a segment in the top trace immediately after HFS. The hyperpolarizing current pulse also resulted in significantly less membrane hyperpolarization compared to pre-HFS hyperpolarizing current pulse. (D) Return to baseline of the apparent input resistance occurred at approximately 6 sec after HFS. (E) Overlay of the membrane response to the hyperpolarizing current pulses before, and immediately after HFS. (F) Magnification of a section of (A) depicting the rebound burst of action potentials due to presumed I_T activation. (G) The stimulation artifacts were manually removed during HFS trace revealing lack of sag current and

rebounds bursting. (H) Graph of the mean ±SEM of the apparent R_{in} before and during HFS (n = 10 relay neurons; $P < 0.001$).

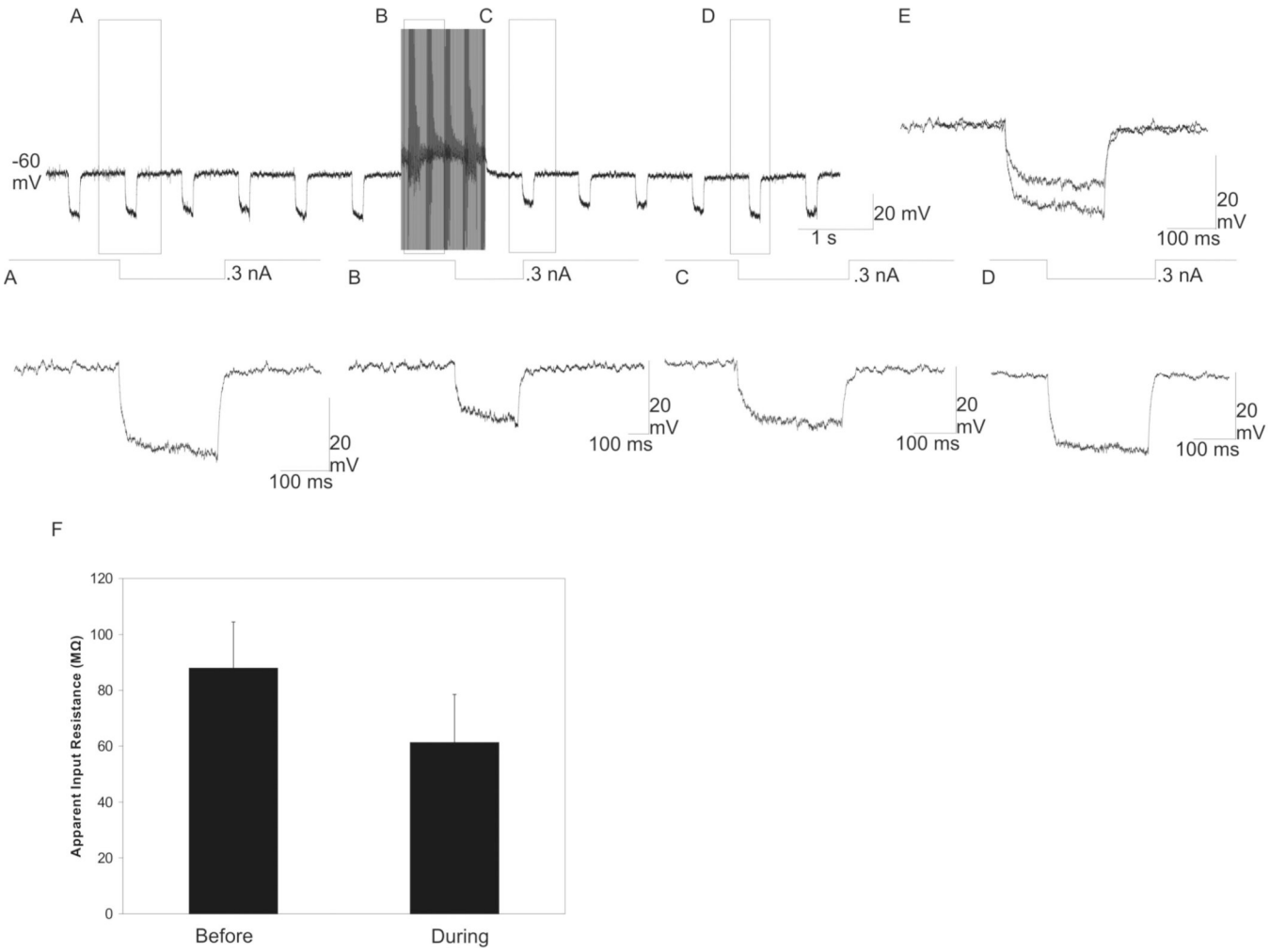

Fig. 5.

Decrease in the apparent input resistance in an nRt/PGN neuron with HFS delivered to the A1 lamina ~600 μm posterior to the recording electrode. Intracellular recording from a nRt/PGN neuron during HFS while hyperpolarizing square-wave current pulses (100–300 ms, 0.3 nA, 1 Hz) are delivered intracellularly to the recorded neuron. (A) Before HFS, the 0.3 nA hyperpolarizing DC resulted in membrane hyperpolarization. (B) Magnification of the labeled portion of the top trace with the stimulation artifacts manually removed. The hyperpolarizing current pulse resulted in significantly less membrane hyperpolarization compared to the pre-HFS hyperpolarizing current pulse. (C) Enlargement of the top trace immediately following HFS. The hyperpolarizing current pulse resulted in significantly less membrane hyperpolarization compared to the pre-HFS hyperpolarizing current pulse. (D) Magnification of top trace following HFS, showing return to baseline apparent input resistance after ~4 seconds post HFS. (E) Overlay of the membrane response to the hyperpolarizing current pulses before and during HFS. (F) graph of the mean ±SEM of the apparent input resistance before and during HFS (87.9 ± 14.8 MΩ and 61.3 ± 15.4 MΩ, respectively; n = 5 nRt/PGN neurons, $P < 0.001$).

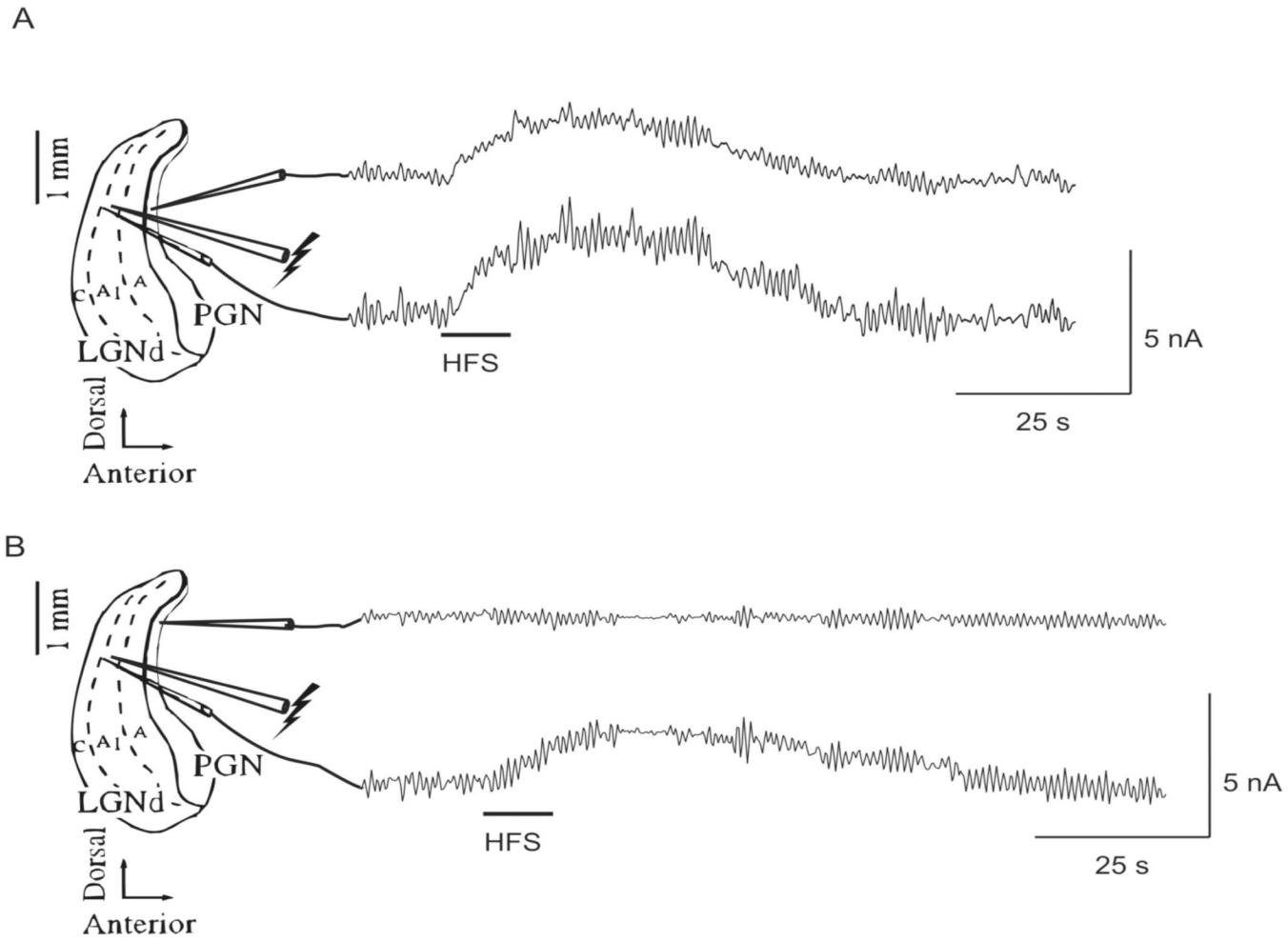

Fig. 6.

Direct measurement of glutamate release in response to HFS (duration ~10 sec, frequency 100 Hz, intensity 300 μA, pulse width 100 μsec) applied to the A1 lamina of the LGN. (A) An increase in oxidation current was recorded simultaneously in the A1 lamina of the LGN (~100 μm anterior to the stimulating electrode) and in the PGN (~600 μm anterior to the stimulating electrode) following HFS (n = 3 slices). (B) When the PGN recording electrode was moved ~500 μm dorsally, no change in oxidation current was recorded in response to HFS, however, an increase in oxidation current was measured in the LGN (n = 3 slices).

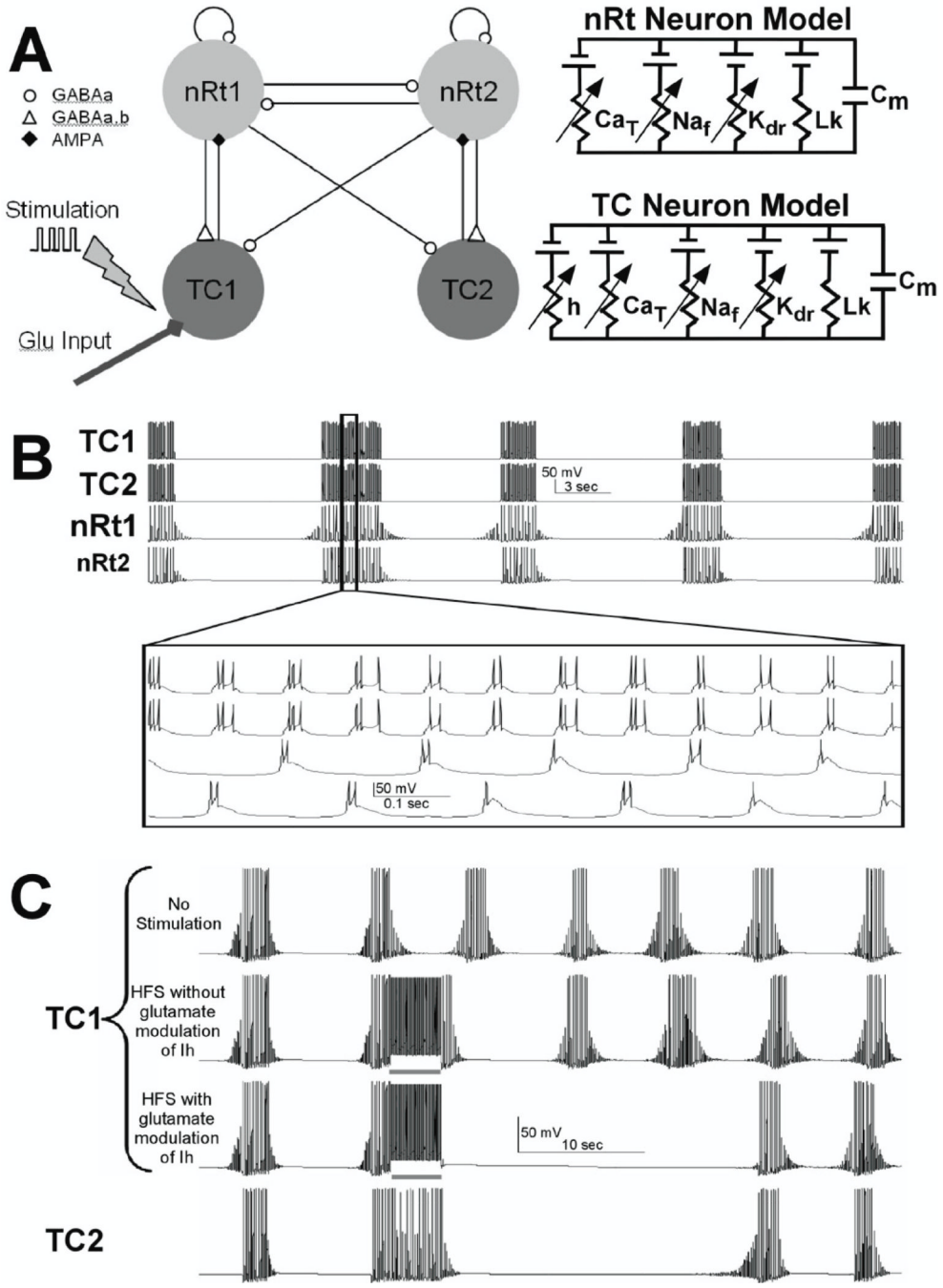

Fig. 7.

Spindling thalamic slice computer model. Two neurons of each type (TC and nRt) constituted the model (A), and HFS and glutamate effects were introduced into the model through the TC neurons. The model produced spindle-like oscillations (B) with reciprocal activation and inhibition between TC and nRt neurons. HFS did not produce any prolonged disruption of the spindle oscillations (C) until glutamate release and glutamate-dependent modulation of I_h were incorporated into the model.